Chemistry & Biology
Article

Prototyping Nanorod Control: A DNA Double Helix Sheathed within a DNA Six-Helix Bundle

Risheng Wang,[1] Wenyan Liu,[1] and Nadrian C. Seeman[1,*]
[1]Department of Chemistry, New York University, New York, NY 10003, USA
*Correspondence: ned.seeman@nyu.edu
DOI 10.1016/j.chembiol.2009.07.008

SUMMARY

The control of the structure of matter is a key goal of nanoscience. DNA is an exciting molecule for control because it forms programmable intermolecular interactions. Stiff DNA structures, such as the double crossover motif, the tensegrity triangle, and the six-helix bundle (6HB) have been used to produce periodic arrays of DNA components. The 6HB motif consists of six DNA double helices flanking an inner cavity whose diameter is similar to that of a double helix. This motif appears to be an excellent candidate to sheathe and control nanorods by inserting them into the cavity, and then to control the placement and orientation of the rod by controlling the DNA sheath. Here, we prototype this kind of control by using a seventh DNA double helix as the nanorod and fixing it inside the 6HB motif.

INTRODUCTION

The control of the structure of matter on the nanoscale is a major goal of many investigators. One route to this target has been the use of the chemical and structural information contained in nucleic acids to build objects, lattices, and devices (Seeman, 2003). The robust structure of the DNA double helix, combined with the specificity and structural predictability of cohesive end association leads to a powerful system for the design and construction of specific structures. DNA nanostructures have been used previously to organize small components, such as metallic nanoparticles (Zheng et al., 2006). This has been done by attaching a single DNA strand to the nanoparticle and then designing that strand to be an inherent component of the DNA motif. Thus, when the DNA binds to the rest of the motif, the nanoparticle is attached to it, and the self-assembly properties of the motif then organize the nanoparticle as well as the DNA.

There is great interest in the organization of 1D rod-like species. Candidates for these species include biological microfilaments or microtubules, as well as carbon nanotubes (CNTs) or other inorganic nanotubes. The idea is that a DNA sheath can be used to organize the contents by interacting with a DNA surface, e.g., a 2D DNA crystal (Winfree et al., 1998) or an origami tile (Yin et al., 2008). Here, we prototype the organization of a 1D species by encapsulating a DNA double helix within a DNA sheath.

A variety of DNA nanotubes have been reported that consist of multiple individual components (Douglas et al., 2007; Ke et al., 2006; Kuzuya et al., 2007; Liu et al., 2004, 2006; Mitchell et al., 2004; Rothemund et al., 2004; Wei and Mi, 2005; Yan et al., 2003; Yin et al., 2008). The six-helix bundle (6HB) DNA motif (Mathieu et al., 2005) (Figures 1A and 1B) is a molecular complex consisting of a cyclic arrangement of DNA double helices that are connected as a specific group of antiparallel double crossover (DX) molecules (Fu and Seeman, 1993), with 120° angles between successive DX components. This arrangement leaves a cavity in the center of the motif (Figure 1A). Long 6HB motifs built by DNA origami methods have been shown to be of value in orienting nuclear magnetic resonance samples (Douglas et al., 2007). Recently, we have shown that it is possible to build a 6HB molecule from two three-domain bent triple crossover motifs (BTX), using lateral cohesive interactions (Kuzuya et al., 2007), in contrast to the usual "sticky-ended" cohesion that brings the ends of double helices together. The BTX units were capable of forming 1D 6HB tubes, either by the addition of sticky ends or by overlapping blunt-ended units (Kuzuya et al., 2007).

Here, we attach another DNA helix to the inside of one of the BTX domains; combined with the second BTX domain, the total construction contains seven helices, including one sheathed in the center (Figures 1C–1E). The strategy, noted above, is the same as used previously to organize metallic nanoparticles: attach the species to be organized to a DNA strand that is an inherent component of the nanostructure. Despite the expected repulsion of the added negative charge at the center, we can encapsulate the seventh helix in the middle of the 6HB sheath. Thus, we are able to prototype the sheathing of a 1D species with a 6HB motif. We demonstrate the sheathing by hydroxyl radical autofootprinting experiments. In addition, we are able to connect the sheathed helices in different molecules by means of traditional sticky ends, thus producing a 1D array that is visible in the atomic force microscope (AFM).

As indicated above, we form the 6HB motif from two different BTX molecules containing a 120° bend between their two DX components; each domain contains six double helical turns. The two BTX molecules join face to face to produce the 6HB motif (Figures 1C and 1D). These two BTX molecules are the blunt-ended unit used previously (Kuzuya et al., 2007), so they can form 6HB motifs but not a 1D tube. Figure 1E is a schematic drawing that shows the seventh DNA duplex

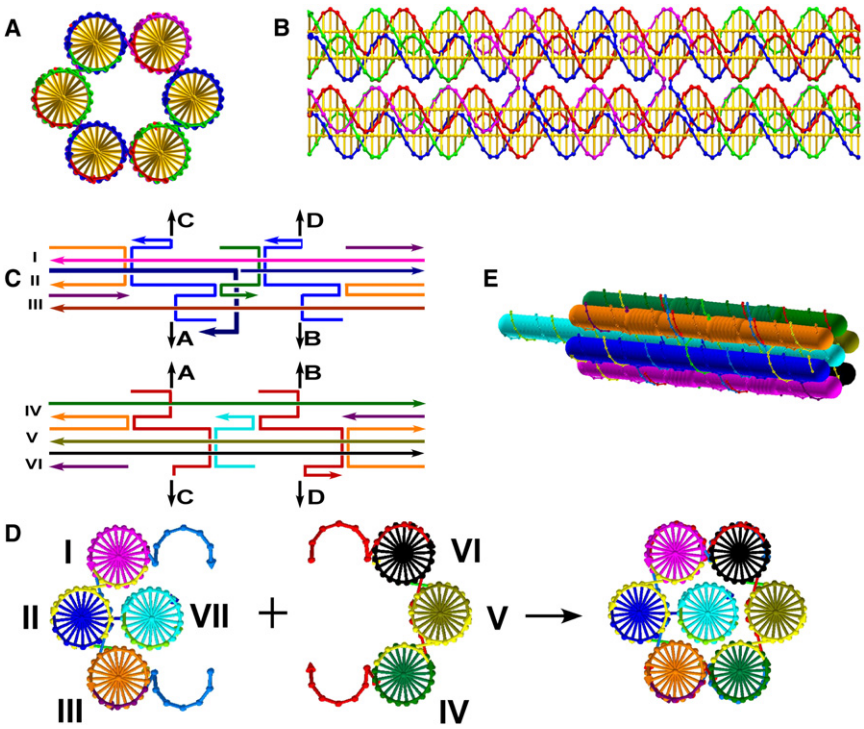

Figure 1. Schematic Drawings of the Motifs Used Here

(A) The top view of DNA 6HB.

(B) The side view of DNA 6HB. These drawings were rendered by GIDEON (Birac et al., 2006).

(C) The BTX molecules. A line drawing indicating the structure of the BTX molecules and the way in which the molecules connect to each other. The helix numbering is shown in Roman numerals. The middle wide dark blue line shows the connection with the seventh helix. Connections between the two BTX molecules are indicated by letters and arrows that connect to the same letters and arrows.

(D) Cross-sectional views of the sheathing process. The guest duplex is connected to the BTX (I, II, and III) molecule. When it is joined with the other BTX molecule, the pair encapsulates the DNA duplex into the middle cavity.

(E) An oblique image to show the sheathing structure.

sheathed within the cavity of a 6HB. Seven colored rods represent the seven DNA helixes. The length of the sheathed seventh duplex is eight turns (84 nt pairs), so that two turns extend beyond the end of the 6HB motif. The seventh helix was held to one of the BTX molecules by 18 nt, which are an inherent component of helix II of BTX (I, II, III) (Figure 1C). We connect the two BTX molecules with four lateral cohesive strands that bridge between them and thereby align the duplex within the central cavity of the 6HB. Figures 1C and 1D schematize the sheathing procedure; we use a slow annealing protocol to form one BTX molecule (I, II, III + VII) in one solution and we form the other BTX molecule (IV, V, and VI) in a separate solution. The two solutions are then mixed in a second step of annealing to yield the sheathed duplex within the 6HB cavity.

RESULTS

We first characterized this structure by nondenaturing polyacrylamide gel electrophoresis (PAGE) (Figure 2). Lane 4 contains the seventh helix without the 18 nt component that attaches it to BTX (I, II, and III), so it contains 150 nt. Lane 3 contains BTX molecule (IV, V, VI); lane 2 contains BTX (I, II, III) including the seventh helix; lane 1 contains the sheath structure of the entire seven helix arrangement. A single sharp band with a mobility similar to that of identically sized marker is taken to represent a well formed DNA nanostructure; counter-indicators would include multimerization, dissociation, and smearing (Seeman, 2002). Lane 2 contains some smearing, possibly owing to the loose connection of the seventh helix, held only by a single tether. Nevertheless, encapsulating the seventh helix within the two BTX molecules aligns it tightly, and a well-formed band is seen in lane 1. As a further control, Figure S3 (available online) shows that a seven-helix complex lacking the C and D cohesive components forms a slower migrating species in addition to the closed sheathed structure; its lower mobility suggests that this new species is likely to be incompletely sheathed.

The hydroxyl radical autofootprinting experiment is a useful way to detect protected regions of DNA strands in solution (Churchill et al., 1988; Seeman, 2002). Hydroxyl radicals cleave DNA by abstracting a hydrogen atom from a deoxyribose sugar in the DNA backbone (Tullius and Dombroski, 1985). The cleavage products are separated using PAGE and then quantitated to show the reactivity of each backbone position. Strands are labeled individually. The pattern of the strand in the complex is compared with the pattern of the strand in a conventional double helix to ascertain changes caused by its being a member of the complex. When analyzing these experiments it is essential that one recognize that the cross-section of the nucleotide pair is not circular: it contains both a major groove and a minor groove that provide a significant volume of solvent accessibility at each step along the helix. Thus, the cylindrical image of the complex shown in Figure 1E is somewhat simplistic: small molecules such as the hydroxyl-radical-generating $Fe(II)EDTA^{2+}$ complex have significant access to the central helix and only a differential protection, relative to an unsheathed helix, can be observed. The sheathed seventh helix contains two parts: six turns protected by the 6HB encapsulation and two further turns exposed outside of the 6HB. The hydroxyl radical autofootprinting data are shown in Figure 3B (the data apply to strand S in Figure 3A). The sheathed strand is shown in red and an unsheathed duplex control is shown in green. There is no protection from the first nucleotide to the twentieth nucleotide, where protection begins. This result is consistent with successful sheathing of the seventh helix. A

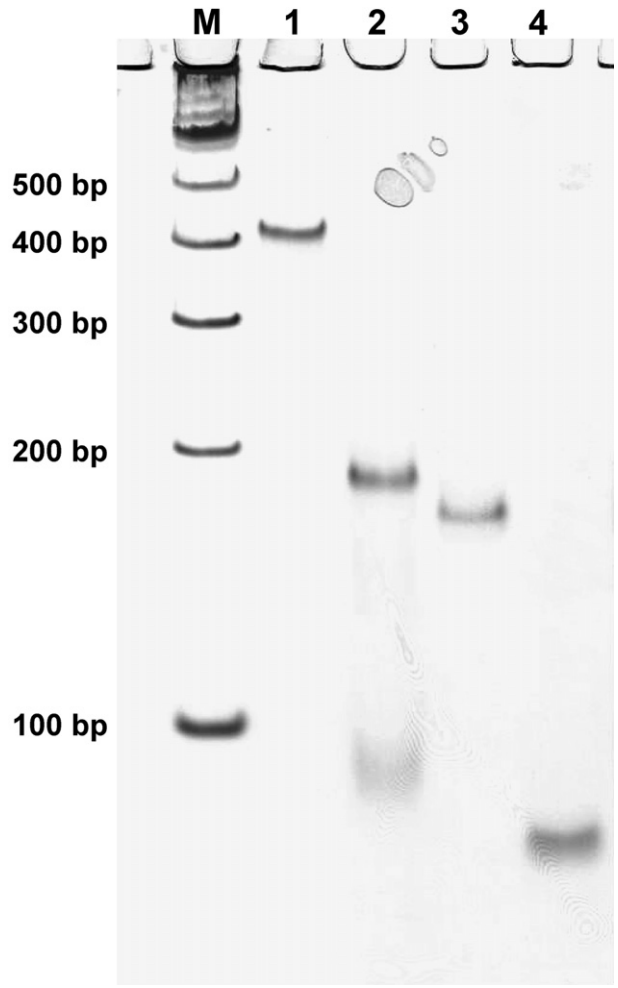

Figure 2. A 6% Nondenaturing Gel Demonstrating Formation of the Sheathing Structure

Lane M contains a 100 bp marker ladder. Lane 1 contains the sheathing structure, with the seventh helix in the central cavity of the 6HB motif. Lane 2 contains the BTX (I, II, III) molecule attached to the seventh helix. Lane 3 contains the BTX (IV, V, VI) molecule. Lane 4 contains only the helix that will be sheathed. It lacks the part of the connecting strand that pairs with residues in helix II of BTX (I, II, III).

gel showing the raw data of the hydroxyl-radical autofootprinting is shown in Figure S4.

Direct visualization of the annealed nanostructure provides further strong evidence for forming the sheathing structure. We extended the seventh helix to 12 turns, so that it reaches 3 turns beyond the 6HB motif in each direction and used it to act as a bridge between complexes, thereby forming 1D arrays of the type shown in the cartoon at the top of Figure 4. From Figures 4A and 4B, we can see clearly the 1D structure connected by the sheathed seventh helices. The height of the sheathed part appears much higher than the helix between sheaths; the sheathed part is between two and three helices thick, but the connecting helix only is a single duplex. The uniformity of the sheathed structures suggests that they are uniform molecules. The 25 nm scale bar in Figure 4A indicates that the sheathed structures are about 15 nm wide; consistent with an ~8 nm sheath when tip convolution is taken into account. The distance between two sheathed helices is consistent with our design (~40.8 nm). Figures 4C and 4D show control images of the four-helix construct consisting of only BTX (I, II, and III) connected by the seventh helix to form a 1D structure. It is clear from these images that the four-helix 1D arrays are not nearly as high as the seven-helix 1D arrays. Figure S4 shows an AFM height analysis of the seven-helix construct and compares it with a four-helix construct (corresponding to the far left structure in Figure 1D) and with a standard 6HB array.

DISCUSSION

We have prototyped sheathing rod-like species within the cavity of the 6HB DNA nanotube. The structure is formed by joining two BTX molecules. The cavity diameter of the 6HB motif, around 2 nm, is of course the same as the diameter of a DNA duplex. The strong repulsion between DNA duplexes has been neutralized by using a high Mg^{2+} concentration (125 mM). The 1D sheathed structure array is shorter than 6HB arrays we reported previously (Mathieu et al., 2005) from 6HB, probably because they are connected only by a single duplex molecule.

The salt conditions required to use DNA as a prototypical nanorod are unlikely to be necessary with other species that do not have such a high density of surface negative charge. However, other modifications to normal ambient conditions within the cavity may be necessary. For example, it may be necessary to increase the hydrophobic character of the cavity interior (Lin et al., 2008) to accommodate species that are not as polar as DNA.

The methodology reported here should open the way to sheath and manipulate rod-like guest species in the future. The key applications are likely to be in the area of biomaterials or bio-inspired materials, rather than directly within a biological context. The only requirement to utilize the capabilities described here is that the guest must have a DNA strand, such as the 5′ end of strand "a" in Figure 3A, that is attached to its tip and that will become a component of the sheathing nanostructure. At this time, it seems likely that CNTs are the most accessible target species. Many species of CNTs are small enough to fit within the 2 nm diameter cavity at the core of the 6HB motif. Replacing the DNA molecule used here with a CNT would need to be done by attaching a single DNA strand to one end of it. Thus the ends two different nanotubes could be attached to, for example, a 2D DNA origami tile at discrete positions, using the 6HB motif as an "adaptor." Numerous attachment methodologies exist (Gu et al., 2009) and can be used not only for attaching the 6HB motif but also for relative orientation and positioning (Rinker et al., 2008). The cavity of the 6HB motif is relatively small, but certainly large enough to encapsulate many species of single-walled CNTs. It is not difficult to increase the radius of the cavity if needed. This can be done by design (Sherman and Seeman, 2006) using either specifically built DNA motifs or methods based on DNA origami (A. Udomprasert, M.N. Bongiovanni, S.L. Gras, and N.C.S., unpublished data).

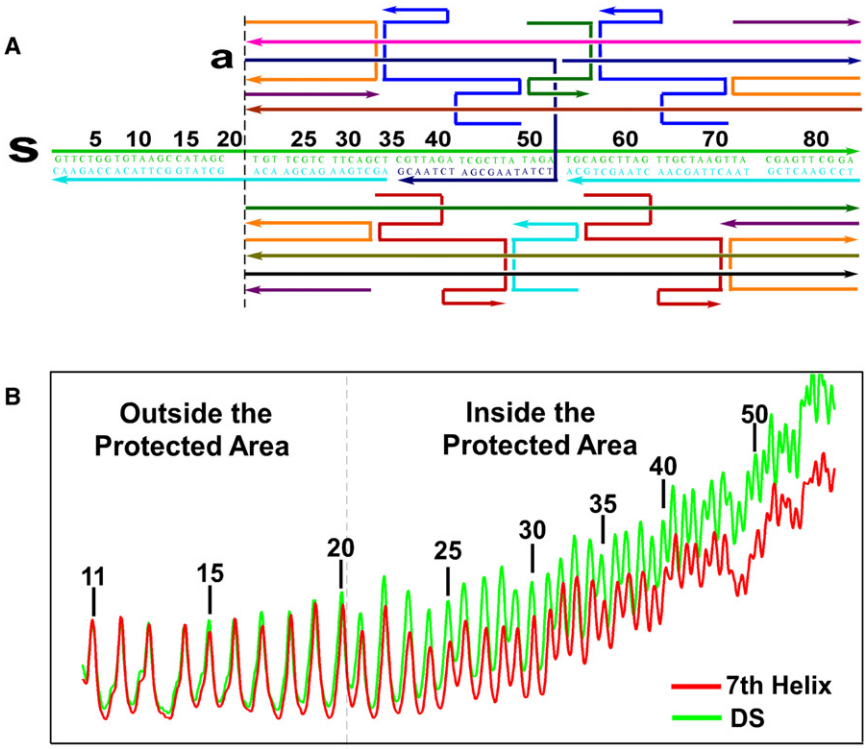

Figure 3. Hydroxyl Radical Autofootprinting Analysis of the Sheathing Structure

(A) The DNA sequence and position labels. Arrowheads indicate the 3′ ends of strands. The sequence of the guest helix and the linear positions are indicated. The strand labeled S is the strand for which hydroxyl radical autofootprinting analysis was performed. The strand labeled "a" is the strand that attaches the guest to the 6HB sheath; note that only the 5′ part of the strand, paired to the rest of the 6HB, would be present if another species were to be sheathed.

(B) Results of the hydroxyl radical autofootprinting analysis. The green line has the data for strand S when it is a control duplex and the red line contains the data for strand S when it is sheathed by the 6HB motif. The dotted line in both panels represents the point where the 6HB motif begins, affording protection to the sheathed helix.

SIGNIFICANCE

The work reported here demonstrates that it is possible to sheathe a nanorod tightly within a DNA nanotube. DNA is readily manipulated and it is easy to direct it to bind in a specific site. If the approach described here is used, a specific site on the nanorod will be placed at a known locus, facilitating the development of specifically sited nanorods. In addition, we have demonstrated that it is possible to fill the gap in a 6HB motif, even though the charge repulsion and the small amount of available cross-sectional space suggests that this might not be possible to do.

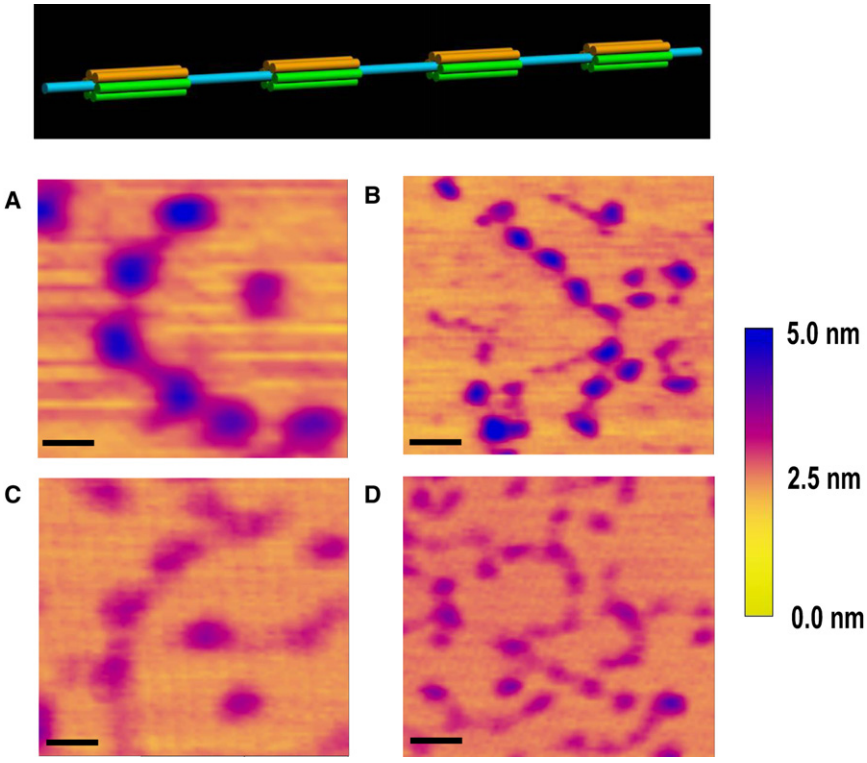

Figure 4. AFM Visualization of the 1D Array Formed by the Sheathing Structure

The top panel is a cartoon showing the 1D array that has been designed, wherein the extensions of the blue sheathed helix are connected to one another.

A and B contain images of this designed 1D array, with the sheathing structures connected by the sheathed helix. At the right is a height bar, indicating the color coding that corresponds to a particular height. Note that the connections go through the middles of the thickened structures, indicating that the sheathed helix is not on the outside of the structure.

C and D contain control images of only the BTX (I, II, and III) molecule connected by partially sheathed helix. Note that the heights of the thickened structures are much lower. The scale bars in A and C are 25 nm and those in B and D are 50 nm.

EXPERIMENTAL PROCEDURES

Sequence Design, Synthesis, and Purification of DNA

The sequences have been designed by applying the principles of sequence symmetry minimization, using the program SEQUIN (Seeman, 1982, 1990). All strands were purchased from Integrated DNA Technologies, Inc. (www.idtDNA.com). DNA strands were purified by 10%–20% denaturing PAGE, eluted in a solution containing 500 mM ammonium acetate, 10 mM magnesium acetate, and 2 mM EDTA from gel, and followed by ethanol precipitation. Sequences are shown in the supplemental data.

Formation of Hydrogen-Bonded Complexes

The complexes were formed by mixing a stoichiometric quantity of each strand, as estimated by OD_{260}, in a solution containing 40 mM Tris, 20 mM acetic acid, 2 mM EDTA, and 125 mM magnesium acetate (TAE/Mg). To prepare 6HB species, the two BTX molecules were annealed separately from 90°C to room temperature in a 2 liter water bath stored in a styrofoam box over the course of 40 hr. In a second step, the two BTX molecules or with the seventh helix were annealed together at 45°C and then cooled in the styrofoam box to room temperature.

Nondenaturing Gel Electrophoresis

Nondenaturing gels contained 6% acrylamide (19:1 acrylamide/bisacrylamide) and the running buffer contained 1× TAE/Mg. The tracking dye containing 1× TAE/Mg, 50% glycerol, and a trace amount of bromphenol blue and xylene cyanol FF was added to the annealed sample buffer. Gels were run on a Hoefer SE-600 gel electrophoresis unit at room temperature. After electrophoresis, the gels were stained with 0.01% Stains-all dye (Sigma-Aldrich) in 45% formamide.

Radioactive Phosphorylation

A 10 pmol portion of each of the DNA strands was dissolved in 20 μl of a solution containing 50 mM Tris-HCl (pH 7.6), 10 mM $MgCl_2$, and 10 mM 2-mercaptoethanol and was mixed with 1 μl of 1.25 mM ^{32}P-ATP (10 mCi/mL) and 2 units of T4 polynucleotide kinase (USB) for 1 hr at 37°C. The reaction was stopped by ethanol precipitation of DNA.

Hydroxyl Radical Analysis

The S strand of the complex was ^{32}P labeled and additionally gel purified from a 10%–20% denaturing polyacrylamide gel. Each of the labeled strands (approximately 1 pmol in 10 μl 1× TAE buffer containing 125 mM Mg^{2+}) was subjected to three different treatments: (1) it was annealed to an excess of unlabeled complementary strand, (2) it was annealed to an excess of a mixture of the other strands forming the complex, or (3) it was treated with sequencing reagents (Maxam and Gilbert, 1977) for a sizing ladder. The samples were annealed as described above. Hydroxyl radical cleavage of the double strand and complex sample took place at 4°C for 2 min (Tullius and Dombroski, 1985), with modifications noted by Churchill et al. (1988). The reaction was stopped by addition of thiourea. The sample was dried, dissolved in a formamide/dye mixture, and loaded directly onto a 10%–20% polyacrylamide/8.3 M urea sequencing gel. Autoradiograms were analyzed on a Storm 860 Gel and Blot Imaging System (GE Healthcare).

Atomic Force Microscopy

A 5 μl sample was spotted onto freshly cleaved mica and the sample was left to absorb for 2 min. To remove buffer salts, 5–10 drops of doubly distilled H_2O were placed on the mica, the drop was shaken off, and the sample was dried with compressed air. All AFM imaging was performed on a Nanoscope IV (Digital Instruments) tapping in air, using commercial cantilevers with silicon tips. Tapping in buffer was tried first, but this 1D structure did not bind well to mica in buffer.

SUPPLEMENTAL DATA

Supplemental Data include five figures and can be found with this article online at http://www.cell.com/chemistry-biology/supplemental/S1074-5521(09)00239-7.

ACKNOWLEDGMENTS

We are grateful to Ruojie Sha for useful discussions about this system and to Thomas D. Tullius for advice about the interpretation of hydroxyl radical cleavage patterns. This research has been supported by grant GM-29544 from the National Institute of General Medical Sciences, grants CTS-0608889 and CCF-0726378 from the National Science Foundation, grants 48681-EL and W911NF-07-1-0439 from the Army Research Office, grant N000140910181 from the Office of Naval Research, and a grant from the W.M. Keck Foundation.

Received: April 9, 2009
Revised: July 15, 2009
Accepted: July 23, 2009
Published: August 27, 2009

REFERENCES

Birac, J.J., Sherman, W.B., Kopatsch, J., Constantinou, P.E., and Seeman, N.C. (2006). Architecture with GIDEON, A program for design in structural DNA nanotechnology. J. Mol. Graph. Model. *25*, 470–480.

Churchill, M.E.A., Tullius, T.D., Kallenbach, N.R., and Seeman, N.C. (1988). A Holliday recombination intermediate is twofold symmetric. Proc. Natl. Acad. Sci. USA *85*, 4653–4656.

Douglas, S.M., Chou, J.J., and Shih, W.M. (2007). DNA-nanotube-induced alignment of membrane proteins for NMR structure determination. Proc. Natl. Acad. Sci. USA *104*, 6644–6648.

Fu, T.-J., and Seeman, N.C. (1993). DNA double-crossover molecules. Biochemistry *32*, 3211–3220.

Gu, H., Chao, J., Xiao, S.-J., and Seeman, N.C. (2009). Dynamic patterning programmed by DNA tiles captured on a DNA origami substrate. Nat. Nanotechnol. *4*, 245–249.

Ke, Y., Liu, Y., Zhang, J., and Yan, H. (2006). A study of DNA tube formation mechanisms using 4-, 8-, and 12-helix DNA nanostructures. J. Am. Chem. Soc. *128*, 4414–4421.

Kuzuya, A., Wang, R., Sha, R., and Seeman, N.C. (2007). Six-helix and eight-helix DNA nanotubes assembled from half-tubes. Nano Lett. *7*, 1757–1763.

Lin, J., Seeman, N.C., and Vaidehi, N. (2008). Molecular dynamics simulations of insertion of chemically modified DNA nanostructures into a water-chloroform interface. Biophys. J. *95*, 1099–1107.

Liu, D., Park, S.H., Reif, J.H., and LaBean, T.H. (2004). DNA nanotubes self-assembled from triple-crossover tiles as templates for conductive nanowires. Proc. Natl. Acad. Sci. USA *101*, 717–722.

Liu, H., Chen, Y., He, Y., Ribbe, A.E., and Mao, C. (2006). Approaching the limit: can one DNA oligonucleotide assemble into large nanostructures? Angew. Chem. Int. Ed. Engl. *45*, 1942–1945.

Mathieu, F., Liao, S., Kopatsch, J., Wang, T., Mao, C., and Seeman, N.C. (2005). Six-helix bundles designed from DNA. Nano Lett. *5*, 661–665.

Maxam, A.M., and Gilbert, W. (1977). New method for sequencing DNA. Proc. Natl. Acad. Sci. USA *74*, 560–564.

Mitchell, J.C., Harris, R., Malo, J., Bath, J., and Turberfield, A.J. (2004). Self-assembly of chiral DNA nanotubes. J. Am. Chem. Soc. *126*, 16342–16343.

Rinker, S., Ke, Y.G., Liu, Y., Chhabra, R., and Yan, H. (2008). Self-assembled DNA nanostructures for distance-dependent multivalent ligand-protein binding. Nat. Nanotechnol. *3*, 418–422.

Rothemund, P.W.K., Ekani-Nkodo, A., Papadakis, N., Kumar, A., Fygenson, D.K., and Winfree, E. (2004). Design and characterization of programmable DNA nanotubes. J. Am. Chem. Soc. *126*, 16344–16352.

Seeman, N.C. (1982). Nucleic acid junctions and lattices. J. Theor. Biol. *99*, 237–247.

Seeman, N.C. (1990). De novo design of sequences for nucleic acid structure engineering. J. Biomol. Struct. Dyn. *8*, 573–581.

Seeman, N.C. (2002). Key experimental approaches in DNA nanotechnology. Curr. Protoc. Nucleic Acid Chem. *12*, 12.1.

Seeman, N.C. (2003). DNA in a material world. Nature *421*, 427–431.

Sherman, W.B., and Seeman, N.C. (2006). Design of low-stress nucleic acid nanotubes. Biophys. J. *90*, 4546–4557.

Tullius, T.D., and Dombroski, B. (1985). Iron(II) EDTA used to measure the helical twist along any DNA molecule. Science *230*, 679–681.

Wei, B., and Mi, Y. (2005). A new triple crossover triangle (TXT) motif for DNA self-assembly. Biomacromolecules *6*, 2528–2532.

Winfree, E., Liu, F., Wenzler, L.A., and Seeman, N.C. (1998). Design and self-assembly of two-dimensional DNA crystals. Nature *394*, 539–544.

Yan, H., Park, S.H., Finkelstein, G., Reif, J.H., and LaBean, T.H. (2003). DNA-templated self-assembly of protein arrays and highly conductive nanowires. Science *301*, 1882–1884.

Yin, P., Hariadi, R.F., Sahu, S., Choi, H.M.T., Park, S.H., LaBean, T.H., and Reif, J.H. (2008). Programming DNA tube circumferences. Science *321*, 824–826.

Zheng, J., Constantinou, P.E., Micheel, C., Alivisatos, A.P., Kiehl, R.A., and Seeman, N.C. (2006). 2D nanoparticle arrays show the organizational power of robust DNA motifs. Nano Lett. *6*, 1502–1504.

